

Enhancement of defect-induced Raman modes at the fundamental absorption edge of electron-irradiated GaAs

R. S. Berg* and P. Y. Yu

Department of Physics, University of California, Berkeley, California 94720
and Center for Advanced Materials, Lawrence Berkeley Laboratory, Berkeley, California 94720

(Received 30 December 1985)

Resonant Raman scattering in electron-irradiated GaAs has been studied. Enhancements in the scattering cross section of both intrinsic and defect-induced phonon modes at the fundamental absorption edge are reported. The experimental results are compared quantitatively with theory. A new scattering mechanism involving elastic scattering between electrons and defects is proposed to explain the resonance of the defect-induced Raman modes.

Resonant Raman scattering (RRS) has been studied extensively in semiconductors ever since dye lasers became commercially available.¹ These studies have mostly concentrated on the intrinsic Raman modes. It is well known that defects can introduce new peaks in the Raman spectra.² In principle, these defect-induced modes should exhibit resonance enhancements like the intrinsic modes. In practice, due to the limited availability of experimental results, our theoretical understanding of the scattering mechanisms and enhancement of defect-induced Raman modes in semiconductors has lagged behind that for intrinsic Raman modes. In this Rapid Communication we present the essential results of a detailed experimental and theoretical study of the enhancement of defect-induced Raman modes in electron-irradiated GaAs. We have used electron irradiation to introduce the defects since this technique tends to produce a more homogeneous distribution of intrinsic point defects in a controllable manner. The deep levels introduced by the high-energy radiations quench the photoluminescence near the absorption edge and make it possible to observe RRS at the band edge.

Our starting material was semi-insulating GaAs grown by the liquid encapsulated Czochralski method. The (110) surface of the sample was irradiated with a beam of 1.6-MeV electrons from a Van de Graaf generator. The electron beam profile was approximately Gaussian with a diameter of

~ 3 mm. The peak intensity of the beam was $\sim 1.1 \times 10^{17}$ cm^{-2} . The defect density at the center of the beam was estimated to be $\sim 5 \times 10^{17}$ cm^{-3} , assuming that the defect introduction rate within the first few mm of the sample is ~ 5 defects/ cm^3 for an incident electron flux of 1 cm^{-2} .³ The Raman spectra were excited by the output of a Styryl-9 dye laser which could be tuned continuously from 1.45 to 1.6 eV. The average output power is typically ~ 200 mW and is focused to a spot of ~ 75 - μm diameter at the center of the irradiated region. The backscattered Raman signal was analyzed and detected by a standard Raman spectrometer. The GaAs sample was cooled to temperatures between 10 and 100 K in an optical Dewar. To obtain the enhancement in the Raman cross sections the measured Raman intensities were corrected for the spectral response of the detector and spectrometer and for the variation in the sample absorption with photon energy (see Fig. 1).

Figure 2 shows the typical Raman spectra of the irradiated GaAs sample. The incident photon frequency was 11944

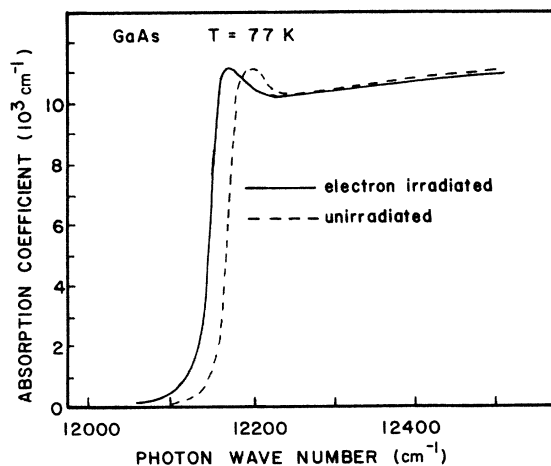


FIG. 1. Absorption spectra of GaAs before and after e irradiation.

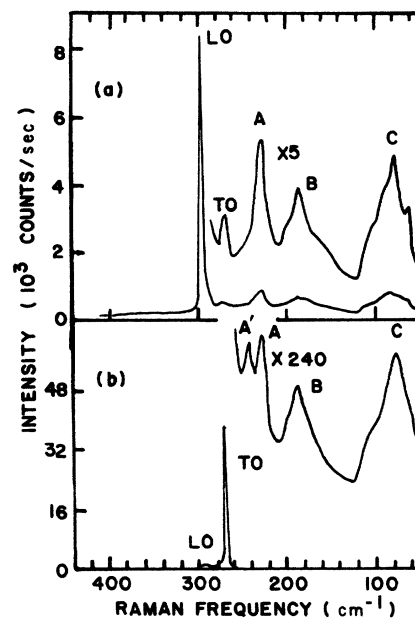


FIG. 2. Raman spectra of e -irradiated GaAs in the two geometries described in the text. In (a) phonons of Γ_1 and Γ_{12} symmetries are allowed. In (b) phonons of Γ_{15} symmetry are allowed.

cm^{-1} . For Fig. 2(a) the incident and scattered radiations were both polarized along the [001] directions so that phonons of Γ_1 and Γ_{12} symmetries were allowed. In Fig. 2(b) the scattered radiation was polarized along the $[1\bar{1}0]$ direction, so only phonons of Γ_{15} symmetry were allowed. Other than for the optical phonons (labeled TO and LO) we also observed four new structures which were absent in the unirradiated samples. These have been labeled *A*, *A'*, *B*, and *C*. A detailed discussion of the identification of these four peaks has been presented elsewhere.⁴ In brief, we have tentatively identified the peaks *A* and *A'* as due to the local vibration mode of an isolated point defect; namely, an As vacancy. The structures *B* and *C* were found to resemble the acoustic phonon density of states in GaAs and therefore were attributed to defect-activated first-order Raman scattering (DAFORS). Similar DAFORS have been reported in ion-implanted GaAs (Ref. 5) and in $\text{Ga}_x\text{Al}_{1-x}\text{As}$ alloys.⁶ Although the identifications of these defect-induced Raman modes are tentative, this turns out to be not crucial in understanding their resonance enhancement.

Our RRS results are presented in Figs. 3 and 4. In Fig. 3 we plot the experimental Raman cross section of the TO phonon obtained in the Γ_{15} scattering geometry (open circles) as a function of the excitation frequency. In Figs. 4(a) and 4(b) we plot the ratio of the peaks *A* and *C* obtained in the scattering geometry of Fig. 2(a) to the cross section of the TO phonon shown in Fig. 3. The enhancement of peak *B* is similar to peak *C* so it will not be shown. The reasons for plotting the relative Raman cross sections rather than the absolute cross sections of these modes are that noise due to day-to-day variations in laser power and optical alignment is minimized. It is obvious from such a plot whether the defect-induced modes have sharper resonance than the TO phonon or not. For comparison we also show in Fig. 4(c) the relative cross section of the symmetry-forbidden LO phonon which is observed in the Γ_1 scattering geometry.

To understand our results we have compared our data first with existing theories of RRS in disorder systems. Shuker and Gammon⁷ have explained Raman scattering in amorphous Si by assuming that momentum conservation is relaxed by disorder. Kawamura, Tsu, and Esaki (KTE) have proposed a specific model to explain DAFORS in

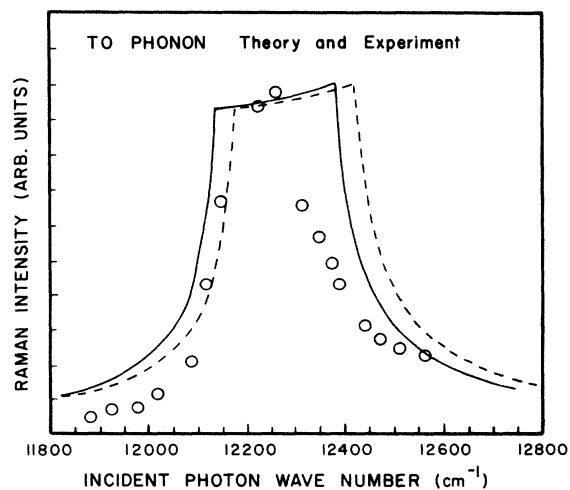


FIG. 3. Enhancement in the TO-phonon cross section.

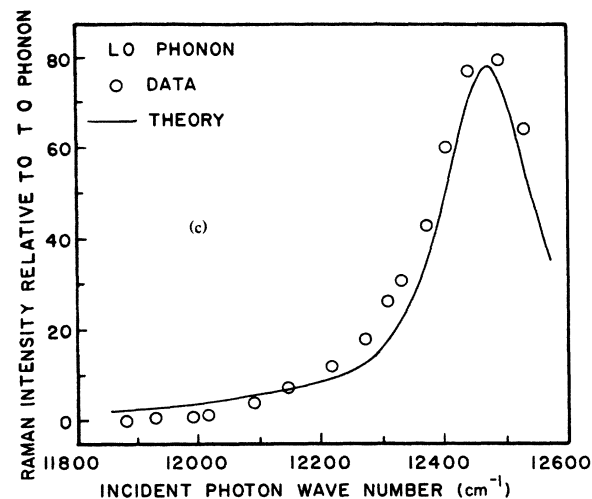
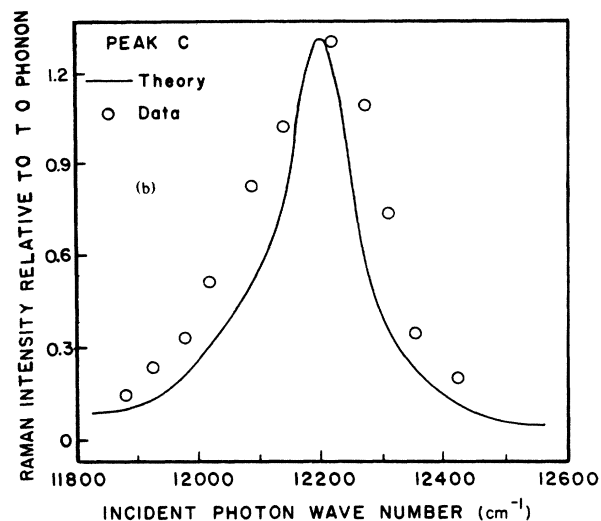
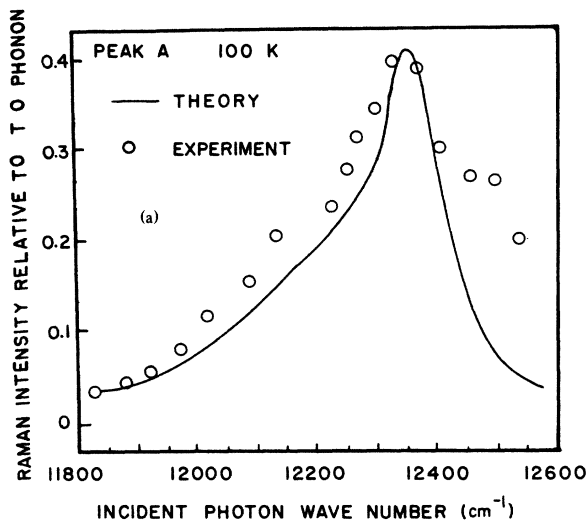


FIG. 4. (a)–(c) Enhancement in the defect-induced Raman modes relative to the TO phonon.

Ga_xAl_{1-x}As alloys in which only the electrons are affected by the disorder, while the phonons are undisturbed. Colwell and Klein⁸ have involved scattering of excitons bound to impurities to explain the breakdown of selection rules of the LO phonon in CdS. More recently, Gogolin and Rashba⁹ have proposed the elastic scattering of excitons by defects to explain the appearance of forbidden phonon modes.

As a starting point we will consider the theory of KTE in which the Raman processes responsible for the defect-activated modes can be represented by Feynman diagrams of the form shown in Fig. 5(a). The main difference between these Feynman diagrams and those for scattering in a perfect crystal is that localized electron-hole states are involved. Through use of perturbation theory the scattering probability *P* for a particular mode with wave vector *q* can be shown to be⁶

$$P(w_i) \propto \left| \sum_{a,b} \frac{\langle f | H_{ER} | b \rangle \langle b | H_{EP} | a \rangle \langle a | H_{ER} | i \rangle}{(w_a - w_i)(w_b - w_s)} \right|^2 \times \delta(w_i - w_s - w_p) \quad (1)$$

where the symbols are defined in Fig. 5(a). To proceed further one has to know the nature of the localized states $|a\rangle$ and $|b\rangle$. In GaAs the binding energies of excitons to impurities are small ($\ll 10$ meV) so at ~ 100 K we do not expect bound excitons to be important. Indeed, the absorption edge of our irradiated GaAs sample in Fig. 1 suggests the existence of band-tail states in which one or both carriers are localized. Following KTE we can assume that the one-particle electron wave functions can be written as a linear combination of a Bloch part $\phi_k(\mathbf{x})$ and a localized part $R_k(\mathbf{x})$, which is a superposition of plane waves

$$R_k(\mathbf{x}) = \int g(\mathbf{k} - \mathbf{k}') \exp(i\mathbf{k}' \cdot \mathbf{x}) d^3k'$$

The lowest-order momentum-nonconserving Raman processes are obtained by the assumption that one of the two electron-hole wave functions $|a\rangle$ and $|b\rangle$ is a localized function. Carrying out the summation over the intermediate states, one obtains in the lowest order the scattering probability

$$P(w_i) \propto \left| \sum_{\mathbf{k}} \frac{C(q)}{[w_{cv}(\mathbf{k}) - w_i][w_{cv}(\mathbf{k}) - w_s]} \right|^2 \delta(w_i - w_s - w_p) \quad (2)$$

where

$$C(q) = \int d^3k_1 \int |R_{ck_1}(\mathbf{x})|^2 e^{i\mathbf{q} \cdot \mathbf{x}} d^3x$$

is the Fourier transform of the perturbation in the electron charge density due to the defects. While this simple theory can explain the presence of DAFORS, it also predicts that the frequency dependence of such processes in the ‘‘vicinity’’ of the energy gap is similar to a symmetry-allowed optical phonon. As a result, the ratio of the DAFORS to the TO-phonon cross section should be independent of the excitation frequency. This is obviously in disagreement with the experimental result shown in Figs. 4(a) and 4(b) for the modes *A* and *C*. Since the enhancement of these modes shows a peak above the absorption edge, one may suggest that defects produce a band of localized states in the absorption continuum and somehow these localized states are

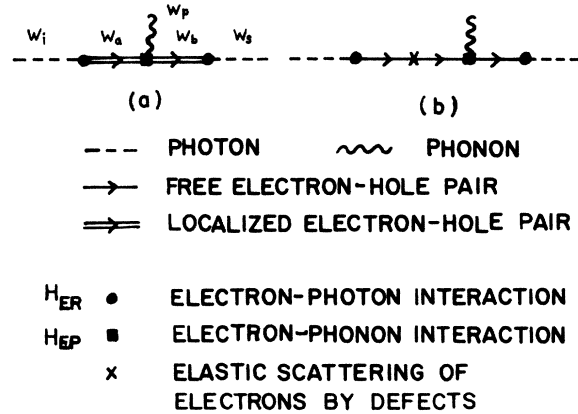


FIG. 5. Diagrammatic representations of the scattering mechanisms responsible for the defect-induced Raman modes. Diagram (a) corresponds to the KTE mechanism, while diagram (b) is the proposed new mechanism involving elastic scattering of electrons by defects.

responsible for the enhancement of modes *A* and *C*, and not the TO phonon. While such an explanation is possible, it is rather unlikely. Since the enhancement peaks for the forbidden LO phonon and the modes *A* and *C* all occur at slightly different phonon energies, it would be necessary to invoke several localized bands to explain them. Instead, we propose that the enhancement peaks of the modes *A*, *C*, and LO phonons occur at frequencies corresponding to the scattered phonons at resonance with the band gap (i.e., these peaks are ‘‘outgoing’’ resonances).

Because of the similarity in the enhancement profile of the *A* and *C* modes and the forbidden LO phonon, we will now consider first the scattering processes responsible for the forbidden LO phonon. Recently, Menendez and Cardona (MC)¹⁰ have demonstrated that there are two possible mechanisms responsible for the forbidden LO phonon in GaAs. The first mechanism is intrinsic and involves third-order perturbation diagrams. The enhancement peak predicted by this mechanism occurs at $w_g + w_p/2$ (where $\hbar w_g$ is the band gap and w_p is the phonon energy), with a width of the order of w_p . The second mechanism is ‘‘extrinsic’’ and involves elastic scattering of electron-hole pairs by defects. This extrinsic mechanism involves fourth-order perturbation diagrams of the kind shown in Fig. 5(b). The enhancement peak predicted by the extrinsic mechanism occurs at $w_g + w_p$, and its width is determined by damping of the electron-hole pair. As found by MC, the extrinsic mechanism can be stronger than the intrinsic mechanism in spite of the fact that it is a higher-order process. The reason is twofold: First, momentum relaxation resulting from the elastic scattering with defects allows double resonance (i.e., both incoming and scattered photons are at resonance) to occur, and second, the electron-LO-phonon (Fröhlich) interaction increases as the square of the phonon wave vector.

To fit our forbidden LO-phonon enhancement to the MC theory, we first determine the energy gap in our electron-irradiated GaAs. From the absorption (Fig. 1) and enhancement of the TO phonon (Fig. 3) we obtain $w_g = 12160 \pm 40$ cm⁻¹. This value of w_g is used to calculate the enhancement of the LO phonon via the extrinsic mechanism of MC [Eq. (A1) in Ref. 10]. The result is

shown as the solid curve in Fig. 4(c). The only adjustable parameters are the peak height and the damping of the electron-hole pair. The damping we obtained (90 cm^{-1}) is somewhat larger than the value of 64 cm^{-1} obtained by Menendez and Cardona at the $E_0 + \Delta_0$ gap. That is expected since our sample has been damaged by electron irradiation. Overall, the agreement between theory and experiment is quite good.

Next we assume that the extrinsic mechanism of MC applies equally well to the defect-induced modes. As in the case of the forbidden LO phonon, the double resonance made possible by elastic scattering with defects can result in the fourth-order processes becoming stronger than the third-order processes of KTE. Since we have no information on peaks' *A* and *C* interaction with electrons, we assumed the electron-phonon matrix element to be constant. By using the phonon energy appropriate for modes *A* and *C* in the theory of MC, we obtain the solid curve in Figs. 4(a) and 4(b). The agreement between theory and experiment is quite satisfactory with no adjustable parameters other than the peak height, although the theory does not reproduce the shoulder on the higher-energy side of the experimental peak for *C*.

A more complete discussion of our theoretical calculations will appear elsewhere.¹¹ In this Rapid Communication it suffices to point out the assumptions which have to be satisfied in order for the fourth-order processes to be dominant. First, the defect concentration should not be so large as to result in multiple scattering of the electron-hole pairs. Such multiple scattering will "localize" the carriers so the KTE mechanism is expected to become dominant for samples with higher-defect concentration. We have, for example,

found that in a neutron-irradiated sample (where the damage is more extensive) the enhancement of the DAFORS mode *C* was different from the electron-irradiated sample and could be explained by the KTE mechanism. Presumably, this is also true in alloys and ion-implanted GaAs. The double resonance in the fourth-order processes is satisfied by phonons of a narrow range of wave vectors around q_0 , where q_0 is defined by $\hbar^2 q_0^2 / 2m \sim \hbar \omega_p$ (m being the electron or hole mass). At the band gap in GaAs q_0 is $\sim 1/10a_0$ (a_0 is the lattice constant of GaAs). However, the frequency of the peak *C* suggested that it involves zone-edge acoustic phonons. To reconcile this difference we must assume that these zone-edge acoustic phonons have enhanced amplitudes around the defects (i.e., they are really resonant modes). At present we have no evidence to support this assumption.

In conclusion, we have found that in electron-irradiated GaAs containing $\sim 5 \times 10^{17} \text{ cm}^{-3}$ of intrinsic defects, the enhancement of the defect-induced Raman modes near the band gap are sharper and stronger than that of the TO phonon. The enhancement profiles can be explained phenomenologically by a fourth-order perturbation theory involving an elastic scattering of the electron-hole pair by defect.

This work was supported by the Director, Office of Energy Research, Office of Basic Energy Sciences, Materials Sciences Division of the U. S. Department of Energy under Contract No. DE-AC03-76SF00098. We are grateful to Dr. D. Goldberg of Lawrence Berkeley Laboratory for assistance in the electron irradiation of the GaAs samples.

*Present address: Department of Physics, Wellesley College, Wellesley, MA 02140.

¹See review articles by R. M. Martin and L. M. Falicov, in *Light Scattering in Solids*, edited by M. Cardona, Topics in Applied Physics, Vol. 8, (Springer-Verlag, Berlin, 1975), p. 50; and by M. Cardona, in *Light Scattering in Solids II*, edited by M. Cardona and G. Güntherodt, Topics in Applied Physics, Vol. 50 (Springer-Verlag, Berlin, 1982), p. 19.

²See, for example, review article by A. S. Barker, Jr., and A. J. Sievers, *Rev. Mod. Phys.* **47**, S1 (1976).

³K. D. Glinchuk, N. S. Zayats, and A. V. Prokhorovich, *Fiz. Tekh. Poluprovodn.* **17**, 751 (1983) [*Sov. Phys. Semicond.* **17**, 471 (1983)].

⁴R. S. Berg, P. Y. Yu, and E. R. Weber, *Appl. Phys. Lett.* **47**, 515 (1985).

⁵S. Ushioda, *Solid State Commun.* **15**, 149 (1974).

⁶H. Kawamura, R. Tsu, and L. Esaki, *Phys. Rev. Lett.* **29**, 1397 (1972).

⁷R. Shuker and R. W. Gammon, *Phys. Rev. Lett.* **25**, 222 (1970).

⁸P. J. Colwell and M. V. Klein, *Solid State Commun.* **8**, 2095 (1970).

⁹A. A. Gogolin and E. I. Rashba, *Solid State Commun.* **19**, 1177 (1976).

¹⁰J. Menendez and M. Cardona, *Phys. Rev. B* **31**, 3696 (1985).

¹¹R. S. Berg, Ph.D. thesis, University of California, Berkeley, California, 1985 (unpublished).